

Spiral CG Deblurring and Fat-Water Separation using a Multi-peak Fat Model

Nicholas Ryan Zwart¹, Dinghui Wang¹, and James Grant Pipe¹

¹Neuroimaging Research, Barrow Neurological Institute, Phoenix, Arizona, United States

Introduction: In spiral imaging, off-resonance due to magnetic field variation and chemical species (such as fat) produce a blurring effect that increases with the sampling window duration. A previously proposed method of simultaneously deblurring and separating the fat and water signal [1-6] was implemented. This algorithm iteratively solves:

$$A^H A x = A^H b, \quad (\text{Eq. 1})$$

where 'A' represents the blurring process, 'H', the conjugate transpose and 'b' represents the gridding-reconstructed image. The conjugate gradient loop iteratively calculates $A^H A$ by using a variable-kernel image space convolution. This method has previously been implemented using a single-peak model for fat signal [1]. **This work proposes** the use of a multi-peak fat signal model using the same framework.

Methods: The proposed multi-peak and single-peak methods were used to reconstruct data of a canola oil-water phantom and in-vivo using a Philips 3T Ingenia platform. The phantom was scanned with a 2D spiral [7] FFE sequence: 55 interleaves, 1x1x4mm res., 300x300 mtx, 80° flip angle, 800ms TR, TE 1.3/2.05/2.8ms, and a 5.24ms sample window. In-vivo data were acquired with a spherically distributed 3D spiral [7, 8] FFE: 40 interleaves, 1x1x2mm res., 300x300x100 mtx, 25ms TR, TE 1.3/1.9/2.9ms, and a 6.13ms sample window. Phantom and in-vivo data were reconstructed in GPI [9] using 8 and 5 iterations of the CG method, respectively. The algorithm runs parallel on the TE and fat-water images.

Results: The phantom data reconstruction time was 1min 40sec and the in-vivo set was 1min 10sec per coil. Figure 1.c shows less residual fat signal in the water image than 1.a. Similar differences are noticeable in-vivo in figure 2.

Conclusion: The multi-peak fat model can be implemented efficiently within the CG deblur and fat-water separation algorithm, requiring no extra processing time over that of the single peak model.

References: [1] Aboussouan, Proc. ISMRM 20, 2012; [2] Bornert, JMRI 32, 2010; [3] Makhijani, IEEE Bio. Imag. Proc., 2006; [4] Fessler, IEEE J. Sig. Proc. 53, 2005; [5] Noll, MRM 25, 1992; [6] Shimakawa, MRM 60, 2008; [7] Pipe, DOI: 10.1002/mrm.24675, 2013; [8] Turley, MRM 70, 2013; [9] Zwart, ISMRM Data Sampling and Reconstruction Workshop, 2013. **Acknowledgements:** Supported by Philips Healthcare.

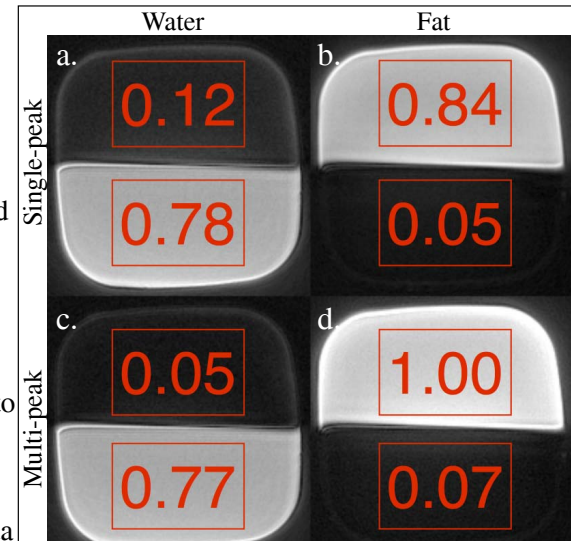


Figure 1. Oil and water phantom reconstructions with average magnitude reported in each ROI. Multi-peak reconstruction (c) shows reduced residual fat signal, compared to the single-peak (a).

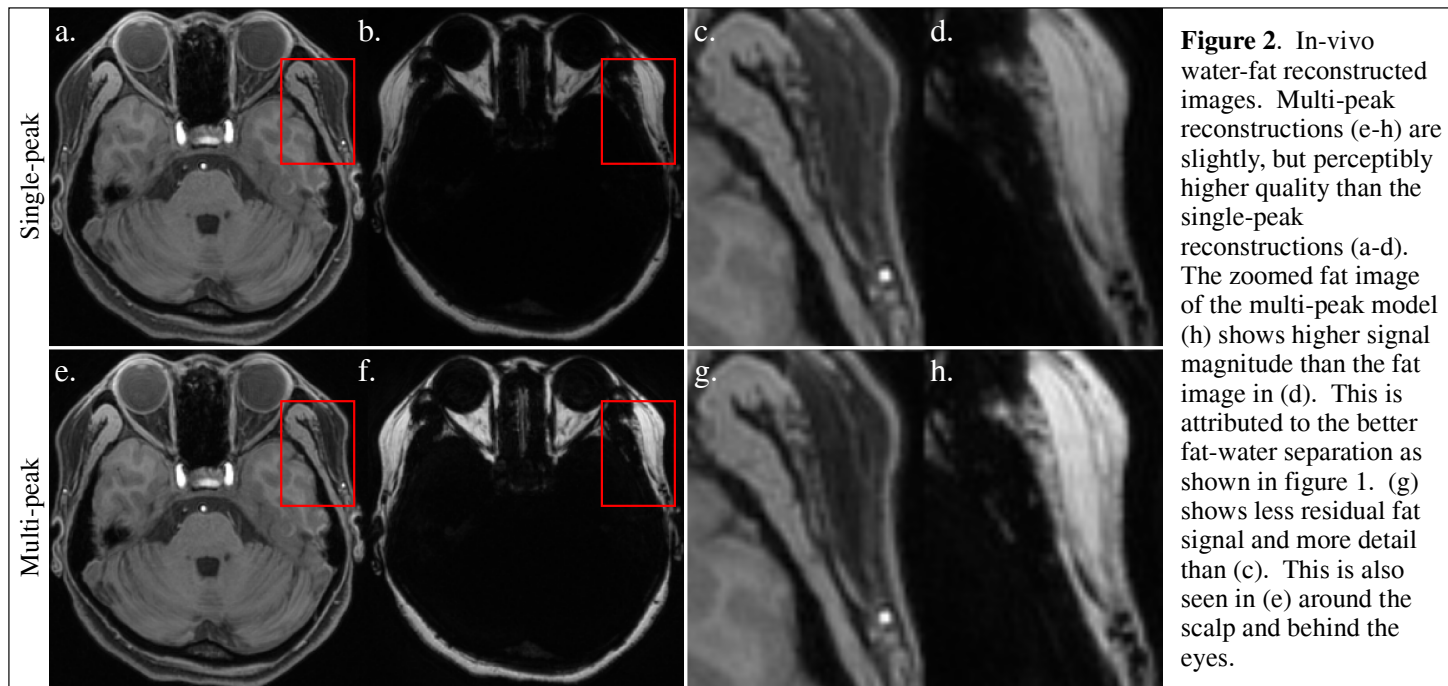


Figure 2. In-vivo water-fat reconstructed images. Multi-peak reconstructions (e-h) are slightly, but perceptibly higher quality than the single-peak reconstructions (a-d). The zoomed fat image of the multi-peak model (h) shows higher signal magnitude than the fat image in (d). This is attributed to the better fat-water separation as shown in figure 1. (g) shows less residual fat signal and more detail than (c). This is also seen in (e) around the scalp and behind the eyes.